JOURNAL OF MATERIALS SCIENCE 33 (1998) 1491–1496

Preparation and characterization of spinel-type Mn–Ni–Co–O negative temperature coefficient ceramic thermistors

J. L. MARTÍN DE VIDALES
Facultad de Ciencias (C-VI), U.A.M., Cantoblanco, 28049 Madrid, Spain

P. GARCÍA-CHAIN
INYSA S.A., c/Aragoneses 9bis, Nave 12, Alcobendas, 28108 Madrid, Spain

R. M. ROJAS*, E. VILA, O. GARCÍA-MARTÍNEZ
Instituto de Ciencia de Materiales de Madrid, Consejo Superior de Investigaciones Científicas, Cantoblanco, 28049 Madrid, Spain
E-mail: rmrojas@icmm.csic.es

Powders of ternary Mn–Ni–Co oxide negative temperature coefficient thermistors were synthesized by a low-temperature alternative route. The procedure allowed straightforward preparation without the addition of any binder, of highly densified Mn–Ni–Co–O semiconducting ceramics as cubic single-phase spinels, at relatively moderate temperature ($\approx 1000\,^{\circ}C$). A tentative cation distribution for the $Mn_{1.5}Ni_{0.6}Co_{0.9}O_4$ spinel oxide has been proposed, and its variation with temperature has also been considered. The dilatometric and X-ray powder diffraction studies carried out for $Mn_{1.5}Ni_{0.6}Co_{0.9}O_4$ showed that sintering takes place in a single stage between 900 and 1000 °C, and yields highly densified ceramic with an apparant density larger than 96% of the calculated X-ray density. Scanning electron microscopy showed different microstructures for the $Mn_{1.5}Ni_{0.6}Co_{0.9}O_4$ spinel oxide, depending on sintering conditions. The value of the sensitivity index, $\beta = 3068$ K, indicates a good technological thermistor performance for this material.

1. Introduction

Certain transition metal compounds that have an element present in more than one oxidation state show electrical conductivity properties. A good example is oxidized nickel oxide, which behaves as a semiconductor, or lithium-doped nickel oxide, in which the concentration of Ni^{3+} depends on the concentration of Li^{+} ions [1]. Controlled valency semiconductors find application as thermistors, that are thermally sensitive resistors. Most of the negative temperature coefficient (NTC) thermistors possess the spinel-type structure; among them oxides formed in the $Ni_xMn_{3-x}O_4$ system have shown very good performances [2]. For these materials to conduct electrically, their spinel octahedral sites must contain at least one element present in two different oxidation states, and those valences must differ by a unit charge [3]. To a first approximation, the semiconducting properties of manganites have been described by a hopping mechanism (electron transfer) between the Mn^{3+} and Mn^{4+} ions in octahedral B sites [4], and the conductivity reaches a maximum when the number of Mn^{3+} ions equals the number of Mn^{4+} ions [2]. It has been demonstrated that in these solids, substitution of manganese for some other cations suitable for tetrahedral A sites occupation (e.g. zinc, magnesium), allows Ni^{2+} to occupy the preferred octahedral B sites, and improves the thermal stability of these solids [5].

Several routes have been proposed for the synthesis of monophase semiconducting ceramics formed in the Mn–Ni–Co–O system. Among them the oxidation at 1000 °C of the rock salt-type Mn–Ni–Co oxide formed at 1400 °C [6], and the thermal decomposition of coprecipitated mixed oxalic precursors [7]. In a previous paper [8] we reported the synthesis at low temperature of tetragonal nickel manganite spinels by coprecipitation of Ni^{2+} and Mn^{2+} cations with a solution of *n*-butylamine. This procedure, that has been used for the synthesis of some other double cubic and/or tetragonal Co–Mn spinel-type oxides [9], yielded very reactive materials [10]. Having this result in mind, we considered it worthwhile to apply the abovementioned procedure to the synthesis of Mn–Ni–Co triple NTC ceramic thermistors. Structural characterization and cation distribution studies have been carried out by X-ray powder diffraction technique. Sintering of materials has been studied by dilatometry

* Author to whom all correspondence should be addressed.

and SEM, and the electrical resistance versus temperature was also measured.

2. Experimental procedure

Manganese, cobalt and nickel in molar ratio Mn : Ni : Co = 1.5 : 0.6 : 0.9 were coprecipitated with *n*-butylamine from an aqueous solution of manganese, nickel and cobalt chlorides. The aqueous amine solution was added slowly with continuous stirring and the pH was kept at ≈ 10.5. A detailed description of the procedure has been reported elsewhere [9]. Precursors with Mn : Ni : Co atomic ratios 1.8 : 1.0 : 0.2; 1.4 : 1.0 : 0.6 and 1.0 : 1.0 : 1.0 and nominal composition $Mn_{2-x}Ni_1Co_xO_4$ ($x = 0.2$, 0.6, 1.0) were also synthesized by the same procedure. Batches of each composition were heated to a specific temperature, kept at that temperature for some time, and then allowed to cool freely in the furnace (see Table I).

X-ray powder diffraction (XRD) patterns were recorded at room temperature on a Siemens D501 diffractometer using monochromatized CuK_α radiation. Diagrams were recorded in the step-scanning mode, with a 0.025° (2θ) step scan and 2 s per step counting time in the range $10° \leqslant 2\theta \leqslant 80°$. Divergence slits located in the incident beam were selected to ensure complete illumination of the specimen surface at 12° (2θ). The least-squares structure refinements were undertaken with the use of the Rietveld program DBWS-9006PC [11]. Rietveld refinements for the single-phase materials were made assuming the space group F*d*3*m* for the cubic spinels. 19 parameters were fitted to the 2801 data points: 1 scale factor, 5 background parameters, the zeropoint for 2θ, 6 profile function parameters (3 for the mixing parameter *m* and 3 for the FWHM), 1 asymmetry correction parameter (for peaks below $2\theta = 50°$), the cell parameter *a*, the oxygen positional parameter *u* and 3 isotropic thermal parameters *B*, 1 for each equiposition 8a, 16d and 32e. The analysis of the microstructure was carried out with a Zeiss scanning electron microscope (SEM) model DSM 960.

Electrical resistance, Ω, versus temperature measurements were carried out in the range −10 to 200 °C. The d.c. resistance was measured with an external voltage source of 1.5 V and a variable external resistance in series with the voltage d.c. source. Electrical measurements were performed on discs of $Mn_{1.5}Ni_{0.6}Co_{0.9}O_4$ and $Mn_{1.8}Ni_{1.0}Co_{0.2}O_4$ materials. Pellets 7.15 mm diameter and 1 mm thick were prepared by hand-press compactation of the precursors previously heated to 200 °C for 5 h. They were then heated to 1000 °C at 30 °C min^{-1}, kept at this temperature for 30 min, and then allow to cool freely in the furnace. No binder was added to the powders. Silver electrodes were painted on two diametrically opposed curved surfaces of the sintered pellets diameter ($\phi \approx 5$ mm, ≈ 0.7 mm thick) with a silver epoxy, and then dried and fired at the appropriate temperature. Ceramics was sealed using proper and clean HC-45/U covers in a clean high-vacuum environment using a cold weld-press. Pellets prepared in this way are referred to as NiO6A ($Mn_{1.5}Ni_{0.6}Co_{0.9}O_4$), and Ni1A ($Mn_{1.8}Ni_{1.0}Co_{0.2}O_4$).

The dilatometric curve was taken with a Netzsch 402E/7 dilatometer in a still-air atmosphere at 5°/10 °C min^{-1} heating/cooling rate. The dilatometric study was carried out on the Mn : Ni : Co = 1.5 : 0.6 : 0.9 precursor previously heated to 500 °C for 3 h, and then isostatically pressed at 2000 kg cm^{-2}.

3. Results and discussion

3.1. X-ray powder diffraction and thermal evolution

The evolution with temperature of the $Mn_{2-x}Ni_1Co_xO_4$ ($x = 0.2$, 0.6, 1.0) and $Mn_{1.5}Ni_{0.6}Co_{0.9}O_4$ powder precursors is identical. The results obtained for the latter are summarized in Table I and Fig. 1. Materials heated to 200, 300 and 400 °C consist of a mixture of poorly crystallized tetragonal $14_1/amd$ and cubic *Fd*3*m* spinel-type phases (Fig. 1a, b). From 500–1000 °C the cubic $Mn_{1.5}Ni_{0.6}Co_{0.9}O_4$ spinel is obtained as a single phase (Fig. 1c–f). The crystallite size increases progressively, and at 1000 °C the K_{α_1,α_2} splitting of the diffraction maxima at $2\theta > 40°$ is observed (Fig. 1f).

TABLE I Thermal treatments, identified phases and cell parameters for tetragonal and cubic nickel manganese spinels with nominal composition $Mn_{1.5}Ni_{0.6}Co_{0.9}O_4$

Temperature (°C)	Time (h)	Identified phases	Cell parameters[a]			XRD figure
			T (tetragonal)		C (cubic)	
			a (nm)	*c* (nm)	a_c (nm)	
200	12	C + T	0.574 1(5)	0.919 0(8)	0.8243(4)	1a
300	6	C + T	0.573 6(4)	0.919 5(7)	0.8261(3)	–
400	6	C + T	0.574 3(2)	0.922 7(4)	0.8288(1)	1b
500	6	C	–	–	0.83217(8)	1c
600	6	C	–	–	0.83403(8)	1d
700	12	C	–	–	0.83465(4)	–
800	16	C	–	–	0.83447(3)	1e
900	12	C	–	–	0.83520(1)	–
1000	12	C	–	–	0.83519(1)	1f

[a] C, cubic spinel-type phase (F*d*3*m*); T, tetragonal spinel-type phase ($14_1/amd$).

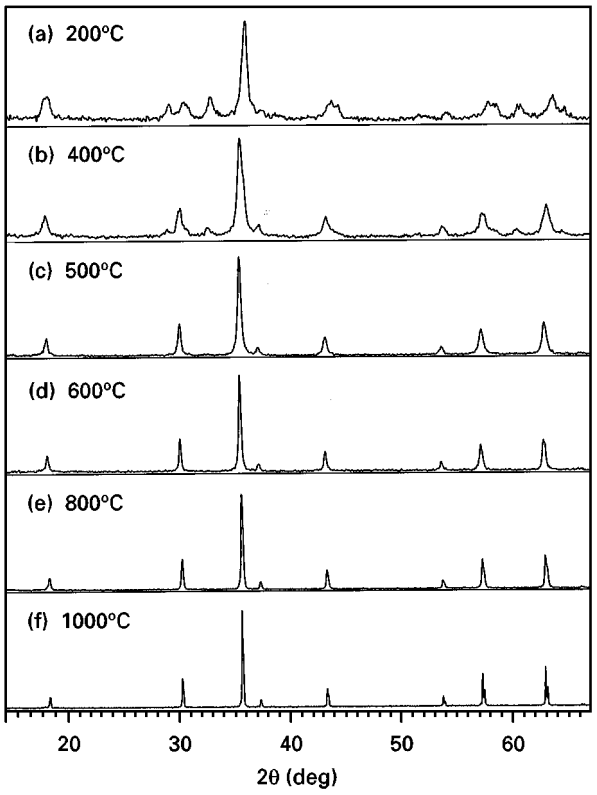

Figure 1 X-ray powder patterns of $Mn_{1.5}Ni_{0.6}Co_{0.9}O_4$ gradually heated to the temperatures indicated and slowly cooled at room temperature.

The cell parameter of the cubic spinel shows a steady increase from 0.832 17(8) nm after heating at 500 °C, to 0.835 19(1) nm after heating at 1000 °C (see Table I).

3.2. Cation distribution and evolution with temperature

A major problem associated to Mn–Ni–Co spinel-type systems is the determination of the valences and cation distribution among the tetrahedral (A sites) and octahedral (B sites) sublattices of the spinel structure.

To put forward a tentative cation distribution for the $Mn_{1.5}Ni_{0.6}Co_{0.9}O_4$ oxide, the relationships pointed out by Poix [12, 13] have been used:

$$a_c = 2.0995 d_A + (5.8182 d_B^2 - 1.4107 d_A^2)^{1/2} \quad (1)$$

where $d_A = \sum n_i (M_i - O)_4$ and $2d_B = \sum n_i (M_i - O)_6$ and the following points have been considered: (i) the $Mn_{1.5}Ni_{0.6}Co_{0.9}O_4$ solid solution shows F$d3m$ cubic symmetry from 500 °C to the upper limit of temperature considered here (1125 °C); therefore it can be inferred that the Mn^{3+} content in B sites is lower than 50% [2]; (ii) according to Dunitz and Orgel [14], Ni^{2+} cannot be situated in A sites; (iii) neutron diffraction studies carried out on nickel manganite spinels $Mn_{3-x}Ni_xO_4$ ($0.57 < x < 1.0$) have shown that the amount of Ni^{2+} in A sites cancels at $x = 0.76$ and remains equal to zero from $x < 0.76$ [15]; (iv) the semiconducting properties of these materials imply the existence of Mn^{3+} and Mn^{4+} ions in octahedral B sites [4]. It is then plausible to propose a cation distribution $(Co^{2+}_{0.9-y}Mn^{2+}_{0.1+y})_A$ $(Ni^{2+}_{0.6}Mn^{4+}_{0.6}Mn^{3+}_{0.8-y}Co^{3+}_y)_B O_4$ with all Ni^{2+} ions located in octahedral B sites, and y ranging from 0–8.

TABLE II Cation–oxygen bond distances [12, 13, 16] used to calculate the unit cell parameters of Co–Mn–Ni cubic spinel with the structural formula shown in Table III

Cation (M)	$(M-O)_4$ (nm)	$(M-O)_6$ (nm)
Mn^{2+}	0.2041	–
Mn^{3+}	–	0.2045
Mn^{4+}	–	0.1843
Co^{2+}	0.1974	–
Co^{3+}	–	0.1892
Ni^{2+}	–	0.2088

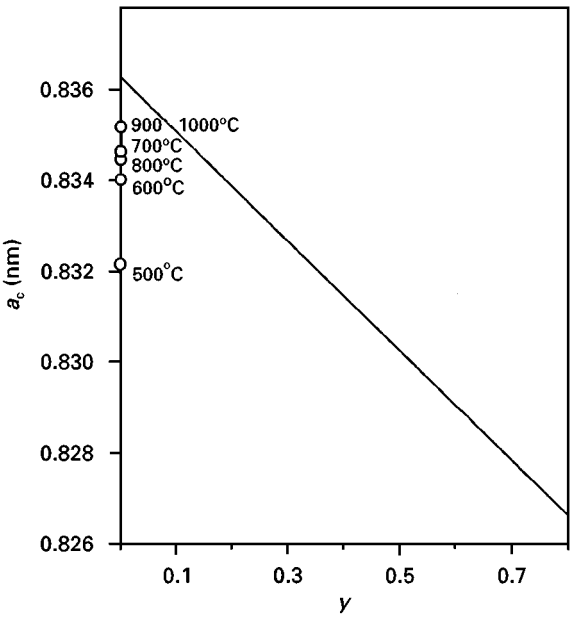

Figure 2 Plot of the calculated a_c versus y for the cation distribution $(Co^{2+}_{0.9-y}Mn^{2+}_{0.1+y})_A(Ni^{2+}_{0.6}Mn^{4+}_{0.6}Mn^{3+}_{0.8-y}Co^{3+}_y)_B O_4$, $0 \leqslant y \leqslant 0.8$. The a_c values were calculated from Equation 1 [11, 12]. (○) Experimental a_c values at different temperatures.

By substituting in Equation 1 the bond distances (d_A, d_B) calculated from data shown in Table II [12, 13, 16], theoretical a_c for each y value can be calculated. The plot of a_c versus y corresponds to the straight line shown in Fig. 2. Theoretical a_c ranges from 0.836 27 nm for $y = 0$ to 0.826 74 nm for $y = 0.8$. From this plot and from the experimental a_c values, the theoretical cation distribution for the cubic $Mn_{1.5}Ni_{0.6}Co_{0.9}O_4$ at each temperature has been calculated (Table III). From 600–1000 °C the theoretical $(Mn^{3+}/Mn^{4+})_B$ ratio is close to the optimum ($Mn^{3+}/Mn^{4+} = 1$) postulated for the maximum for conductivity [17].

3.3. Sintering process

Pellets of the $Mn_{1.5}Ni_{0.6}Co_{0.9}O_4$ and $Mn_{1.8}Ni_{1.0}Co_{0.2}O_4$ precursors were submitted to the same thermal treatments as the powders, and XRD patterns recorded after each treatment were similar to those of the powders. The crystallinity increased progressively between 500 and 900 °C, and from

TABLE III Experimental unit cell parameter, proposed cation distribution, $(Mn^{4+}/Mn^{3+})_B$ and $(Mn^{2+}/Co^{2+})_A$ ratios for manganese–nickel–cobalt $(Co^{2+}_{0.9-y}Mn^{2+}_{0.1+y})_A(Ni^{2+}_{0.6}Mn^{4+}_{0.6}Mn^{3+}_{0.8-y}Co^{3+}_{y})_BO^{2-}_4$ cubic spinels at different temperatures

Temperature (°C)/ time (h)	Cell parameter, a_c (nm)	y values in the structural formula	$(Mn^{3+}/Mn^{4+})_B$	$(Mn^{2+}/Co^{2+})_A$
500/6	0.832 17(8)	0.345	0.75	0.80
600/6	0.834 03(8)	0.19	1.01	0.41
700/12	0.834 65(4)	0.135	1.11	0.31
800/16	0.834 47(3)	0.15	1.08	0.33
900/12	0.835 20(1)	0.09	1.18	0.23
1000/12	0.835 19(1)	0.09	1.18	0.23

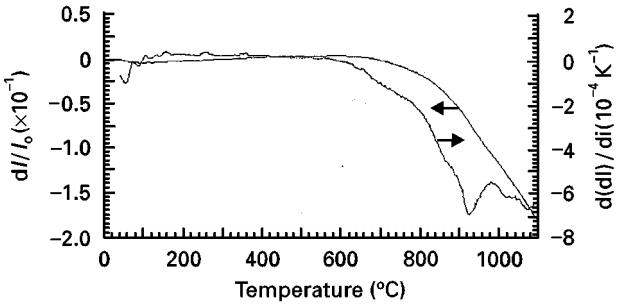

Figure 3 Dilatometric curves of $Mn_{1.5}Ni_{0.6}Co_{0.9}O_4$ spinel previously heated at 500 °C for 3 h.

900–1000 °C it improved dramatically: the K_{α_1,α_2} splitting of the diffraction maxima at $2\theta > 40^\circ$ are easily observed in patterns recorded at the latter temperature. The pellet significantly shrinks between 900 and 1000 °C. While from 200–900 °C the diameter of the $Mn_{1.5}Ni_{0.6}Co_{0.9}O_4$ disc decreases from 7.15 mm to 6.43 mm, between 900 and 1000 °C it diminishes to 5.43 mm. The pycnometric apparent density of the sintered NiO6A and Ni1A pellets gave values greater than 96% of the calculated X-ray density.

The dilatometric curve recorded for $Mn_{1.5}Ni_{0.6}Co_{0.9}O_4$ is shown in Fig. 3. In the temperature

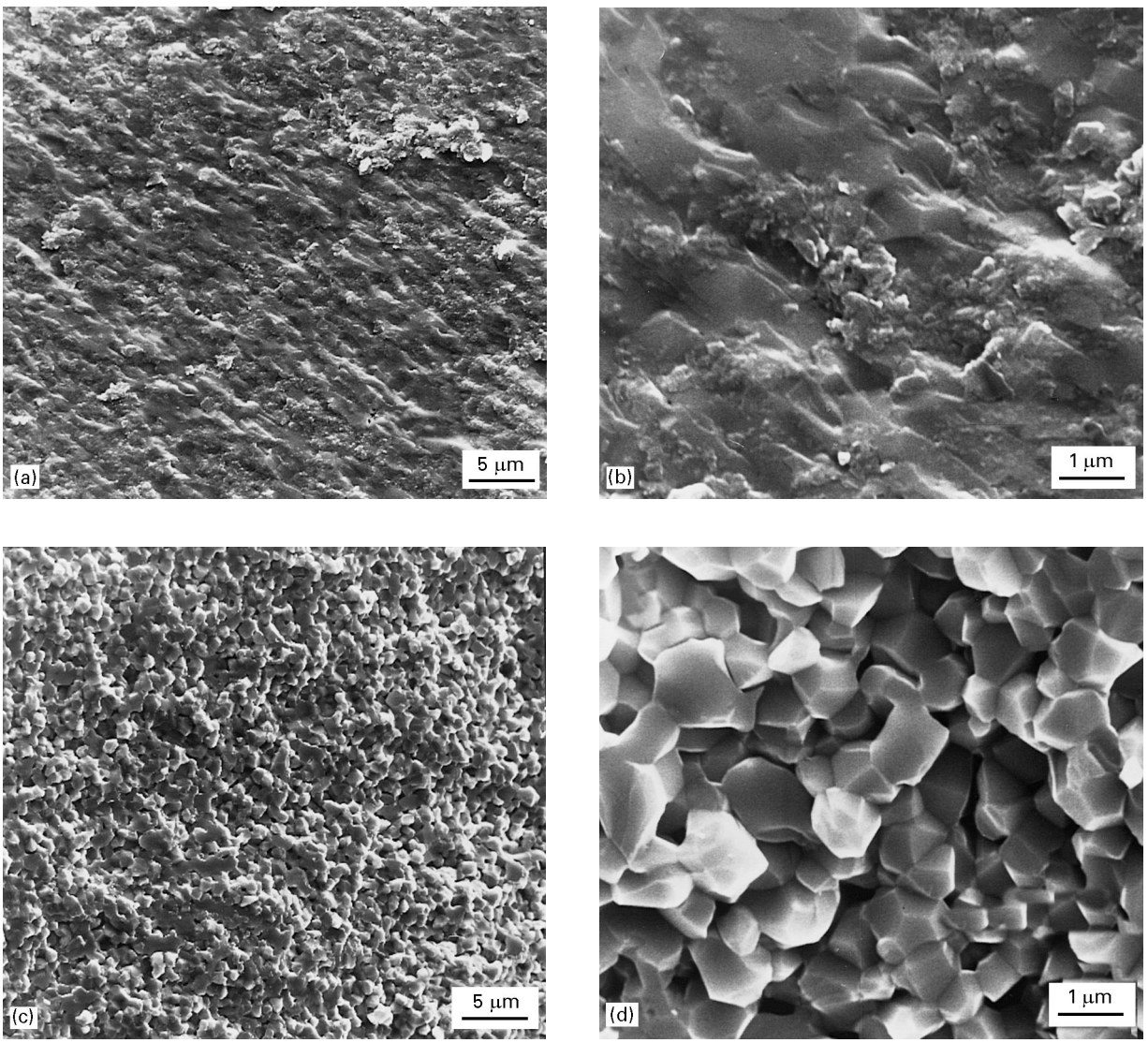

Figure 4 Scanning electron micrographs taken on a fresh fracture of $Mn_{1.5}Ni_{0.6}Co_{0.9}O_4$ spinel: (a, b) hand-pressed NiO6A disc; (c, d) disc from the dilatometric study.

range 600–1100 °C, a pronounced step is observed. ($\Delta l/l_0 = -17\%$). This step is related to the sintering of the ceramic and to the crystal growth of the spinel phase, that has been detected by X-ray diffraction (Fig. 1d–f).

Fig. 4 shows scanning electron micrographs taken on fresh fractures of two different pellets of $Mn_{1.5}Ni_{0.6}Co_{0.9}O_4$. The first two pictures (Fig. 4a, b) were taken on a fresh fracture of the sintered hand-pressed NiO6A pellet. Micrographs shown in Fig. 4c, d were taken on a fresh fracture of the disc from the dilatometric study (Fig. 3). At this point it is worth remembering that, for the dilatometric study, powders of $Mn_{1.5}Ni_{0.6}Co_{0.9}O_4$ precursor were previously heated to 500 °C for 3 h, and then isostatically pressed at 2000 kg cm^{-2}. Differences between both microtextures are evident. In the first case, an almost continuous surface without any pores or cracks is observed, and neither grain boundaries nor individual particles can be distinguished. Pictures taken on the second disc (Fig. 4c, d) show a very homogeneous distribution of discrete particles of approximately 1 μm. A detailed study of the influence of the sintering conditions on the microtexture of the $Mn_{1.5}Ni_{0.6}Co_{0.9}O_4$ material is actually in progress.

3.4. Electrical measurements

Measurements of the electrical resistance, Ω, versus temperature was carried out on the two encapsulated discs of $Mn_{1.5}Ni_{0.6}Co_{0.9}O_4$ (NiO6A) and $Mn_{1.8}Ni_{1.0}Co_{0.2}O_4$ (Ni1A) described in Section 2. In Fig. 5 the resistance, Ω, versus T plots for $Mn_{1.5}Ni_{0.6}Co_{0.9}O_4$ and $Mn_{1.8}Ni_{1.0}Co_{0.2}O_4$ materials are shown. It can be observed that in the range of temperature measured, the resistance decreases progressively as the temperature increases (see inset of Fig. 5).

The sensitivity index, β, which is one of the most important characteristics of technical interest for thermistors, is given by the equation $\beta = \ln R_1 - \ln R_2/(1/T_1 - 1/T_2)$. In the present case, for the $Mn_{1.5}Ni_{0.6}Co_{0.9}O_4$ and $Mn_{1.8}Ni_{1.0}Co_{0.2}O_4$ spinels, the values of β in the temperature range −10 to 200 °C (263–473 K), are 3068 and 3804 K, respectively. These values are within the requirements of the industry (2800–4820 K) for NTC thermistors.

4. Conclusion

The synthesis procedure reported here constitutes a very convenient alternative route for the preparation of ternary Mn–Ni–Co oxide thermistors. It allows the straightforward preparation without the addition of any binder, of highly densified Mn–Ni–Co–O spinels as single phase, at relatively moderate temperature (≈ 1000 °C). The values of the $(Mn^{3+}/Mn^{4+})_B$ ratio between 600 and 1000 °C calculated from the proposed cation distribution, is close to the optimum postulated for the maximum of conductivity. The values of the sensitivity index, β, indicate good technological thermistor performances.

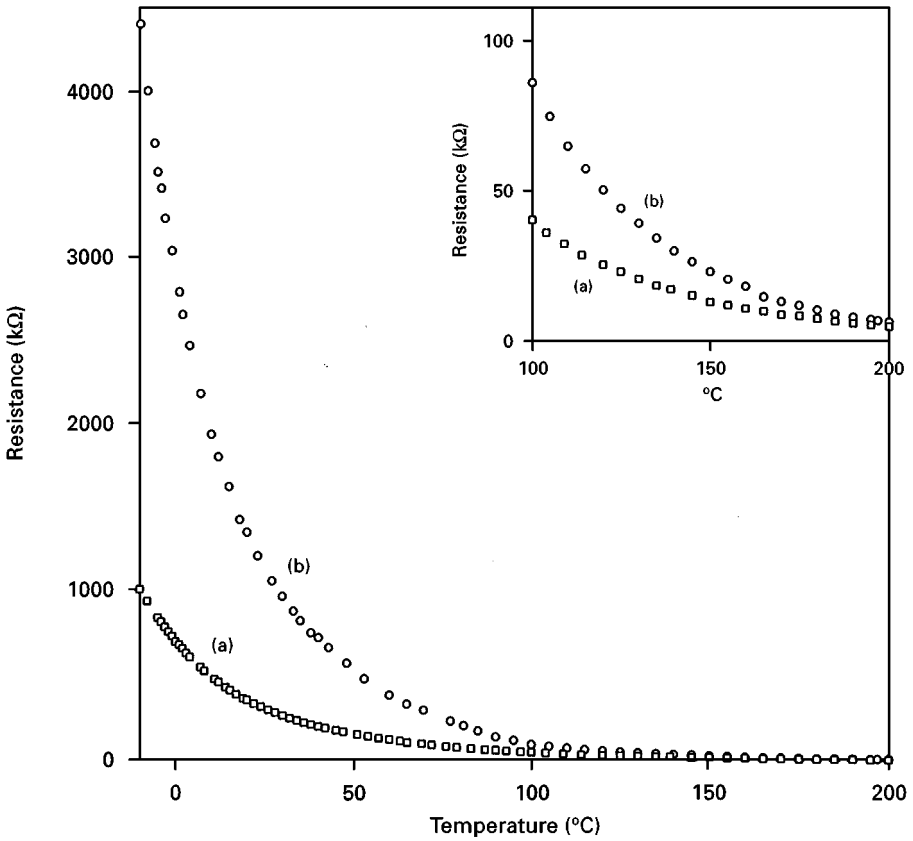

Figure 5 Resistance versus temperature plots of (a) $Mn_{1.5}Ni_{0.6}Co_{0.9}O_4$ and (b) $Mn_{1.8}Ni_{1.0}Co_{0.2}O_4$ thermistors. The inset shows an enlarged area of the 100–200 °C region.

Acknowledgements

The authors thank Drs P. Duran and C. Moure, Instituto de Ceramica y Vidrio (CSIC), for the dilatometric measurement. This work was supported by ClCyT Project MAT94-0799.

References

1. A. R. WEST, in "Solid state chemistry and its applications" (Wiley, New York, 1984) p. 734.
2. R. LEGROS, R. METZ and A. ROUSSET, *J. Mater. Sci.* **25** (1990) 4410.
3. E. D. MACKLEN, *J. Phys. Chem. Solids* **47** (1986) 1073.
4. E. G. LARSON, R. J. ARNOTT and D. G. WICKHAM, *ibid.* **23** (1962) 1771.
5. J. TÖPFER and A. FELTZ, *Solid State Ionics* **59** (1993) 249.
6. T. MEGURO, T. YOKOHAMA and K. KOMEYA, *J. Mater. Sci.* **27** (1992) 5529.
7. T. BATTAULT, R. LEGROS, A. BEAUGER, E. FOLTRAN and A. ROUSSET, *Ann. Chim. Fr.* **20** (1995) 403.
8. J. L. MARTÍN DE VIDALES, R. M. ROJAS, E. VILA and O. GARCÍA-MARTÍNEZ, *Mater. Res. Bull.* **29** (1994) 1163.
9. J. L. MARTÍN DE VIDALES, O. GARCÍA-MARTÍNEZ, E. VILA, R. M. ROJAS and M. J. TORRALVO, *ibid.* **28** (1993) 1135.
10. E. VILA, R. M. ROJAS, J. L. MARTÍN DE VIDALES and O. GARCÍA-MARTÍNEZ, *Chem. Mater.* **8** (1996) 1078.
11. A. SAKTHIVEL and R. A. YOUNG, in "Users Guide to Programs DBWS-9006 and DBWS-9006PC for Rietveld Analysis of X-ray and neutrons Powder Diffraction Patterns" (School of Physics, Georgia Institute of Technology, Atlanta, CA, 1995).
12. P. POIX, *Bull. Soc. Chim. Fr.* **5** (1965) 1085.
13. *Idem*, *C.R. Acad. Sci. (Paris)* **268** (1969) 1139.
14. J. D. DUNITZ and L. E. ORGEL, *J. Phys. Chem. Solids* **3** (1957) 20.
15. B. GILLOT, J. L. BAUDOUR, F. BOUREE, R. METZ, R. LEGROS and A. ROUSSET, *Solid State Ionics* **58** (1992) 155.
16. A. ROUSSET, F. CHASSAGNEUX and P. MOLLARD, *C.R. Acad. Sci. (Paris)* **279** (1974) 1129.
17. A. GILLOT, M. KHARROUBI, R. MELZ, R. LEGROS and A. ROUSSET, *Solid State Ionics* **44** (1991) 275

Received 24 March
and accepted 23 October 1997